Empirical Mode Decomposition in a Time-Scale Framework

Marcelo A. Colominas
Lab. Señales y Dinámicas no Lineales,
Fac. de Ingeniería - UNER
CONICET, Argentina
Email: macolominas@bioingenieria.edu.ar

Gastón Schlotthauer
Lab. Señales y Dinámicas no Lineales,
Fac. de Ingeniería - UNER
CITER - CONICET, Argentina
Email: gschlotthauer@conicet.gov.ar

***Abstract*—The analysis of multicomponent signals, made of a small number of amplitude modulated - frequency modulated components that are overlapped in time and frequency, has gained considerable attention in the past years. These signals are often analyzed *via* Continuous Wavelet Transform (CWT) looking for ridges the components generate on it. In this approach one ridge is equivalent for one mode. The Empirical Mode Decomposition (EMD) is a data-driven method which can separate a signal into components ideally made of several ridges. Unfortunately EMD is defined as an algorithm output, with no analytical definition. It is our purpose to merge the data-driven nature of EMD with the CWT, performing an adaptive signal decomposition in a time-scale framework. We give here a new mode definition, and develop a new mode extraction algorithm. Two artificial signals are analyzed, and results are compared with those of synchrosqueezing ridge-based decomposition, showing advantages for our proposal.**

I. Introduction

The analysis of signals made of the superposition of a small number of components modulated both in amplitude and frequency (AM-FM) has received considerable attention in the past decades. This attention particularly increased in the past few years, not only because of a theoretical interest but also because of the versatility of these *multicomponent signals* to model phenomena such as audio signals [1], biomedical signals [2], or economic temporal series [3].

The separation problem becomes non-trivial when the modes are overlapped both in time and frequency in such way that no simple linear filtering is able to recover them. If they occupy however disjoint domains in a time-frequency or time-scale plane, they can be isolated by applying either a Short-Time Fourier Transform (STFT) or a Continuous Wavelet Transform (CWT) and look for the *ridges* the modes generate on such representations [4], [5], [6]. From this perspective it results in one mode for every ridge.

On the other hand, the Empirical Mode Decomposition (EMD) [7] is a data-driven method which works directly on the observation domain. It considers oscillations at a local level, decomposing a signal into a small number of so-called intrinsic mode functions (IMFs), which are basically signals symmetrically oscillating around zero that can be modulated in amplitude and frequency. In some cases, the EMD decomposition matches better to physics and/or perception when two close tones are considered as a whole, as in the beat effect [8]. Therefore, EMD does not rely on the idea of one mode for every ridge. For this technique, the components can be something more complex than circular functions, thus gaining more versatility.

Nevertheless, EMD is defined as an algorithm output, with no analytical definition. Because of that, and in order to provide it with a more solid mathematical framework, it is the main purpose of this paper to merge the data-driven nature of EMD with the solid mathematical grounds of the time-scale representations. The paper is organized as follows. We give a brief introduction to EMD and the problem of the local mean in Sec. II. The CWT and synchrosqueezing are discussed in Sec. III. Our proposal is described in Sec. IV, while numerical experiments and its results are presented in Sec. V. Sec. VI concludes the present work.

II. Empirical Mode Decomposition and the Local Mean Problem

Empirical Mode Decomposition (EMD) is an adaptive (data-driven) method to analyze non-stationary signals stemming from nonlinear systems. It produces a local and fully data-driven separation of a signal in fast and slow oscillations. Working in a deflationary scheme, in the first step the analyzed signal $x(t)$ is decomposed into

$$x(t) = d_1(t) + a_1(t), \tag{1}$$

with $d_1(t)$ being an IMF, the part of the signal that *locally* oscillates faster, and $a_1(t)$ begin the first *local mean*. The method continues decomposing the local mean as $a_1(t) = d_2(t) + a_2(t)$, and so on. At the end, the original signal can be expressed as a sum of IMFs ($d_k(t)$, $k = 1 \dots K$) plus a final trend ($a_K(t)$)

$$x(t) = \sum_{k=1}^{K} d_k(t) + a_K(t). \tag{2}$$

The EMD algorithm can be summarized as follows [7], [9]:

1) identify the local extrema of $x(t)$
2) interpolate between minima (resp. maxima) to obtain the lower (resp. upper) envelope $e_{min}(t)$ (resp. $e_{max}(t)$)
3) compute the local mean $a(t) = (emin(t) + emax(t))/2$
4) extract the detail $d(t) = x(t) - a(t)$

978-0-9928-6265-7/16/$31.00 ©2016 IEEE

5) iterate on the residue $a(t)$

The whole thing reduces to the separation of a signal into mode plus local mean, as in Eq. (1) (or as in step 4), and then repeat the same procedure on the local mean (step 5). Given the difficulties of a definition for a local mean, the creators of EMD defined it as the mean of the upper and lower envelopes found through spline interpolations of the corresponding local extrema. This geometric definition, although useful in practice, lacks of preciseness thus making difficult the analytical study of EMD. An analytical proposal can be found in [10], where the local mean $a(t)$ of a signal $x(t)$ is given by

$$a(t) = \frac{1}{\alpha(t)} \int x(u) w\left(\frac{t-u}{\alpha(t)}\right) du, \tag{3}$$

where $w(u)$ is a unitary mass weighting function concentrated around zero and $\alpha(t)$ is the *local scale*. The author of [10] considered that the choice of $w(u)$ is not necessarily difficult but the choice of the local scale $\alpha(t)$ is a delicate problem. One must notice however the similarity of Eq. (3) with a *scaling function* analysis evaluated at the local scale:

$$L_x^{\varphi}(t,s) = \frac{1}{s} \int x(u) \varphi\left(\frac{t-u}{s}\right) du, \tag{4}$$

where the scaling function $\varphi(u)$ plays the role of weighting function. Then,

$$a(t) = L_x^{\varphi}(t, \alpha(t)). \tag{5}$$

III. Continuous Wavelet Transform and Synchrosqueezing

Let us introduce the continuous wavelet transform

$$W_x^{\psi}(t,s) = \frac{1}{s} \int x(u) \psi^*\left(\frac{t-u}{s}\right) du, \quad s > 0, \tag{6}$$

where $\psi(u)$ is an *analytic wavelet* and z^* stands for the complex conjugate of z. The vertical reconstruction formula reads

$$x(t) = \frac{2}{\widetilde{C_\psi}} \mathcal{R}e\left(\int_0^{\infty} W_x^{\psi}(t,s) \frac{ds}{s}\right) \tag{7}$$

with $\widetilde{C_\psi} = \int \hat{\psi}^*(f) \frac{df}{f}$, where $\hat{\psi}(f) = \int \psi(u) e^{-2\pi i f u} du$ is the Fourier transform of $\psi(u)$.

The synchrosqueezing [11], [6], a special case of reassignment [12], aims at sharpen the representation, improving its readability, while remaining invertible. Here, instead of the more popular scale to frequency mapping, we apply a scale to scale mapping by using

$$\hat{s}(t,s) = \frac{2\pi i W_x^{\psi}(t,s)}{\partial_t W_x^{\psi}(t,s)}, \tag{8}$$

defined only for points in $B = \{(t,s) / \partial_t W_x^{\psi}(t,s) \neq 0\}$. Then, the synchrosqueezed CWT reads

$$T_x(t,s) = \int_B W_x^{\psi}(t,v) \delta(s - \hat{s}(t,s)) \frac{dv}{v}, \tag{9}$$

while the reconstruction formula becomes

$$x(t) = \frac{2}{\widetilde{C_\psi}} \mathcal{R}e\left(\int_0^{\infty} T_x(t,s) ds\right). \tag{10}$$

For practical implementations we follow [5]. A binning of the scale is defined $\{s_k\}_{k=0}^{\infty}$ and then the intervals $\mathcal{S}_k = [\frac{s_k + s_{k-1}}{2}, \frac{s_k + s_{k+1}}{2}]$. The synchrosqueezing is approximated by $\widehat{T_x}(t, s_k) = \int_{s:|\hat{s}(t,s)| \in \mathcal{S}_k} W_x^{\psi}(t,v) \frac{dv}{v}$ and the reconstruction is $x(t) = \frac{2}{\widetilde{C_\psi}} \mathcal{R}e\left(\sum_k \widehat{T_x}(t, s_k)\right)$.

The synchrosqueezing framework defines a special class of components and how they are mixed [6].

Definition 3.1: Intrinsic Mode Type Functions (IMT)[1]. A continuous signal $x(t) \in \mathbb{R}$, $x \in L^{\infty}(\mathbb{R})$ is an IMT with accuracy $\epsilon > 0$ if $x(t) = A(t)\cos(2\pi\phi(t))$, with A and ϕ having the following properties: $A \in C^1(\mathbb{R}) \cap L^{\infty}(\mathbb{R}), \phi \in C^2(\mathbb{R}), \inf_t \phi'(t) > 0, \sup_t \phi'(t) < \infty$, and for all t $A(t) > 0, \phi'(t) > 0, |A'(t)|, |\phi''(t)| \leq \epsilon \phi'(t)$.

Definition 3.2: Superposition of well-separated IMTs. A function $x(t) \in \mathbb{R}$ consists of well-separated intrinsic mode components, up to accuracy ϵ, and with separation D, if there exists a finite number K such that $x(t) = \sum_{k=1}^{K} A_k(t)\cos(2\pi\phi_k(t))$, where all the components are IMT and their phase functions ϕ_k satisfy for all t: $\phi_k'(t) > \phi_{k-1}'$ and $|\phi_k'(t) - \phi_{k-1}'(t)| \geq D[\phi_k'(t) + \phi_{k-1}'(t)]$.

An important theorem from [6] ensures the CWT of an IMT has most of its non-zero coefficients confined to a "ribbon" around its local scale.

Theorem 3.1: If $d(t) = A(t)\cos(2\pi\phi(t))$ is an IMT with accuracy ϵ, and $\psi(t)$ is an analytic wavelet compactly supported in frequency with $\operatorname{supp}\hat{\psi} \subseteq [f_\psi - \Delta, f_\psi + \Delta]$, then $|W_d^{\psi}(t,s)| > \epsilon^{1/3}$ only when $(t,s) \in Z = \left\{(t,s) / |s - \frac{f_\psi}{\phi'(t)}| < \frac{\Delta}{\phi'(t)}\right\}$.
(The ribbon is actually around $f_\psi/\phi(t)'$, where f_ψ is the peak of the wavelet Fourier spectrum.)

Finally, the mode extraction amounts at find a ridge by solving [2]

$$\max_{c(t)} \int E_x(t,s) dt - \lambda \int [c'(t)]^2 dt, \tag{11}$$

where $E_x(t,s) = \log(|T_x(t,s)|^2)$, and $\lambda > 0$ is the regularization parameter. Then, the mode is estimated as

$$d(t) = \int_{|s - c(t)| < \frac{\Delta}{f_\psi} c(t)} T_x(t,s) ds. \tag{12}$$

Unlike other approaches based on synchrosqueezing, we define here a variable "ribbon width" which suits better to the scale-dependent resolution of wavelet-based methods. For the extraction of more than one mode, a deflationary strategy is

[1]The definitions from [6] are for complex signals. Since we are interested on real signals, we slightly modify the definitions keeping however all of its essence

[2]The actual implementation is on a discretized ridge $c(n)$. We use the Synchrosqueezing Toolbox [13] that implements a heuristic (greedy) approach that maximizes the objective at each time index, assuming the objective has been maximized for all previous time indices.

usually applied: once the mode is extracted, its ribbon on the time-scale representation is zeroed, and the next ridge extraction is performed [14]. With these criteria, the modes do not necessarily appear ordered by scale or frequency.

IV. Proposed Algorithm

A. A New Definition for a Mode

We propose here to define a mode, i.e. the part that locally oscillates faster, of a given signal taking Eq. (5) as inspiration but focusing on the mode instead of the local mean. If the local mean is the result of a scaling function analysis evaluated at a specific local scale, then the mode is the result of the integration of a wavelet analysis from the finest scale to the mentioned local scale. Combining Eqs. (1) and (5) with the reconstruction formula (7), we obtain:

$$d(t) = \frac{2}{\widetilde{C_\psi}} \mathcal{R}e \left(\int_0^{C\,\alpha(t)} W_x^\psi(t,s) \frac{ds}{s} \right), \tag{13}$$

where $\alpha(t)$ is the local scale, and C a real constant later explained. This idea explicitly implements the mode extraction as a time-dependent high-pass filtering, widely discussed on the EMD literature [9], [15].

B. The Local Scale

For the definition of the local scale we use the following estimate:

Estimate 4.1: Let $d(t)$ be an IMT, and t_0 and t_1 two consecutive local extrema of $d(t)$. Then, provided ϵ is sufficiently small,

$$\frac{1}{2\phi'(t_0)} + \frac{1}{2\phi'(t_1)} \approx 2(t_1 - t_0). \tag{14}$$

Sketch of the proof. The estimation is easily verified for a pure tone. For the general case, we start by taking first order Taylor approximation of $\phi(t)$ around both t_0 and t_1 (since ϵ is small enough we can ignore the terms quadratic onwards):

$$\begin{aligned} \phi(t) &\approx \phi(t_0) + \phi'(t_0)(t - t_0) \\ \phi(t) &\approx \phi(t_1) + \phi'(t_1)(t - t_1) \end{aligned} \tag{15}$$

Evaluating every approximation on the other extrema, and adding member to member, we get

$$(\phi(t_1) - \phi(t_0)) \left(\frac{1}{\phi'(t_0)} + \frac{1}{\phi'(t_1)} \right) \approx 2(t_1 - t_0). \tag{16}$$

Next, applying the condition $d'(t^*) = 0$, which holds for $t^* = t_0$ and $t^* = t_1$, leads to

$$\begin{aligned} \phi(t_1) - \phi(t_0) = \frac{1}{2\pi} \Bigg[\pi + \arctan \left(\frac{A'(t_1)}{2\pi A(t_1)\phi'(t_1)} \right) \\ - \arctan \left(\frac{A'(t_0)}{2\pi A(t_0)\phi'(t_0)} \right) \Bigg]. \end{aligned} \tag{17}$$

Since both arguments of the arctangent functions are $O(\epsilon)$ because of the bound on $|A'(t)|$ given by IMT definition (Def. 3.1), it is demonstrated that $\phi(t_1) - \phi(t_0) \to 1/2$ as $\epsilon \to 0$. □

This estimate tell us that we can approximate the mean of the local scale in two consecutive local extrema as twice the time distant between them. We also use the local extrema of $x(t)$ as estimations of those of the mode $d(t)$ [16], [17]. Therefore we can define

$$\alpha(t) = 2(t_{\ell+1} - t_\ell), \quad t_\ell < t < t_{\ell+1}, \tag{18}$$

where $\{t_\ell\}$ are the local extrema of $x(t)$. This idea dates back from the original EMD contribution [7], where it is stated that "*...the characteristic time scale is defined by the time lapse between the extrema...*". It is also mentioned in [18], where the term *empiquency* was coined.

C. Discontinuity Problems and Synchroqueezing

Our piecewise constant estimation of the local scale might cause some discontinuity problems for the mode $d(t)$. In order for $d(t)$ to be continuous at t_0 (local extremum of $x(t)$) it should be $d(t_0) = \lim_{t \to t_0} \frac{2}{\widetilde{C_\psi}} \mathcal{R}e \left(\int_0^{C\,\alpha(t)} W_x^\psi(t,s) \frac{ds}{s} \right)$, which can be guaranteed if $W_x^\psi(t_0, s) = 0$, for $\min(\alpha(t_0^-), \alpha(t_0^+)) < s < \max(\alpha(t_0^-), \alpha(t_0^+))$. This is hardly the general case. Therefore, synchrosqueezing must be used. The synchrosqueezed CWT being a "sharped" version contains less non-zero coefficients, while every mode domain becomes "smaller". We end up with

$$d(t) = \frac{2}{\widetilde{C_\psi}} \mathcal{R}e \left(\int_0^{C\,\alpha(t)} T_x(t,s) ds \right). \tag{19}$$

D. The Constant C

As for the constant C, we must look at Thm. 3.1. For an IMT, the "ribbon" in its CWT is $[\frac{f_\psi - \Delta}{\phi'(t)}, \frac{f_\psi + \Delta}{\phi'(t)}]$. Since we are only interested in the coarse-scale (therefore low-frequency) border, and $\alpha(t)$ is an approximation of the instantaneous scale $1/\phi'(t)$, then $C = f_\psi + \Delta$ is the right choice.

E. Local Scale Refinement

We must take into account the fact that the local extrema of $x(t)$ are estimations of those of the real unknown mode $d(t)$. After applying Eq. (19), the extrema of this *proto*-mode are closer to those of the real mode than the extrema from signal $x(t)$. Therefore we can use them to perform a refinement on $\alpha(t)$, and again estimate the mode $d(t)$ from the synchroqueezed CWT of $x(t)$. This procedure is similar to that of EMD's *sifting*, but while on EMD its consists on successive local mean extractions, here we use it only as a way to improve the selection of the characteristic points to define the local scale. This is congruent with some interpretations of sifting as a better selection of characteristic points [10].

This refinement can be performed until a certain criterion, such as $\frac{2}{\widetilde{C_\psi}} \mathcal{R}e(\int_0^{\alpha_d(t)} T_d(t,s) ds) / ||d(t)||^2$ being smaller than certain threshold and the number of extrema of $d(t)$ remain the same as those of $x(t)$. Here we emphasized that the local scale was estimated from the *proto*-mode.

F. Border Treatment

Our proposal presents border issues caused by the same causes of those ef EMD. The local scale defined in Eq. (18) is incomplete, because it is not defined between the left border and the first local extremum, and between the last extremum and the right border. Mirroring the extrema close to the borders leads to good results.

V. Experimental Results

For our experiments we used the *bump wavelet*, characterized by its Fourier transform

$$\hat{\psi}(f) = e^{1-\frac{1}{1-\left(\frac{f-f_\psi}{\Delta}\right)^2}} \chi_{[f_\psi-\Delta, f_\psi+\Delta]}, \tag{20}$$

which is compactly supported and admits a unique peak at $f = f_\psi$. For the central frequency, we use $f_\psi = 0.5$, which is the maximum normalized frequency for a discrete-time signal. The scale resolution is conditioned by the parameter Δ. We achieved good results with $\Delta = 0.25$. We apply a deflationary scheme: once the signal is decomposed in $x(t) = d_1(t) + a_1(t)$, the decomposition continues on $a_1(t)$. We compare our results with those based on ridge detection. For this task we use the algorithm from [13] with default parameters, and Eq. (12) for mode estimation.

A. Superposition of AM-FM overlapped components

As a first example we present a typical case of AM-FM components overlapped in both time and frequency. The discrete-time signal $x(n) = x_1(n) + x_2(n) + x_3(n)$ is composed of $x_1(n) = \cos\left(2\pi\left(\frac{15}{256}n + \frac{9000}{512\pi}\sin\left(\frac{2\pi}{1000}n\right)\right)\right)$, $x_2(n) = \cos\left(2\pi\left(\frac{15}{768}n + \frac{9000}{1536\pi}\sin\left(\frac{2\pi}{1000}n\right)\right)\right)$, and $x_3(n) = \exp\left(-\pi\left(\frac{n-1000}{250}\right)^2\right)\sin\left(2\pi\frac{3}{256}n\right)$, for $n = 1\ldots2000$, with a separation of $D \approx 1/3$ according to Def. 3.2.

The results can be appreciated in Fig. 1. The left panel shows the ridge-based decomposition, with several "jumps" from one ridge to another. In the right panel, the refinement of the local scale is evident after only three iterations. The mean square errors for our method are: 6.9×10^{-4}, 2.3×10^{-3} and 1.3×10^{-3} respectively for modes first and second and residue. The modes are superimposed with the true components, which appear in dashed red. The errors for the ridge-detection based method are: 2×10^{-2}, 2.5×10^{-2} and 4.9×10^{-3}.

B. Nonlinear waveforms

As a second example we present a superposition of a triangular wave whose wavelength shortens one after another in a "linear chirp" manner, and an actual linear chirp of the form $c(n) = \cos(2\pi 2 \times 10^{-5} n^2)$ for $n = 1\ldots2000$. The results are presented in Fig. 2. The triangular waveform generates more than one ridge in the time scale representation. The ridge-based mode extraction algorithm would scattered the waveform into several modes (it would find at least three ridges) and may also ignore the fine-scale (high frequency) information, as we can see on the left panel of Fig. 2. These limitations of the algorithms that rely on the one ridge - one mode paradigm are currently tackled by new proposals,

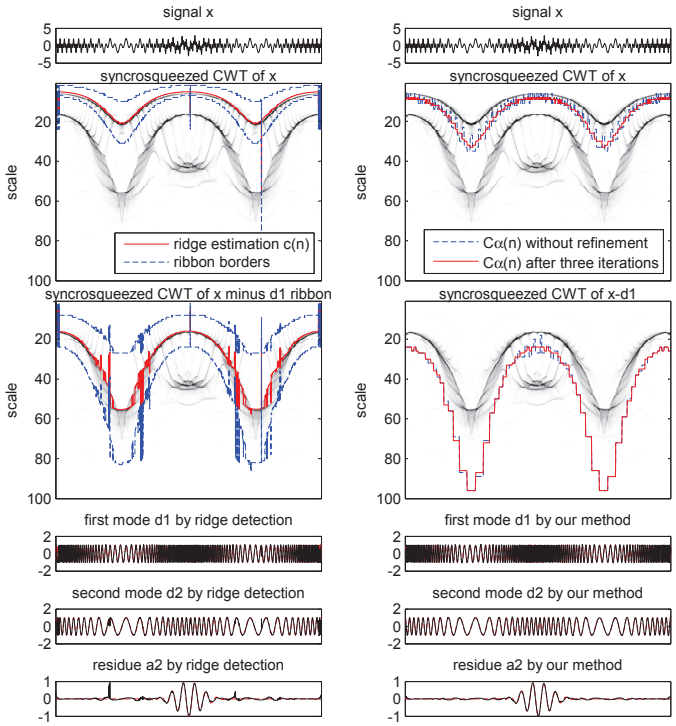

Fig. 1. Superposition of AM-FM components. Left panel: ridge-based method. Right panel: our proposal. Top to bottom: signal $x(n)$, synchrosqueezed CWTs of $x(n)$ and that for the second step, and the first two modes and residue in black superimposed with the true components in dashed red.

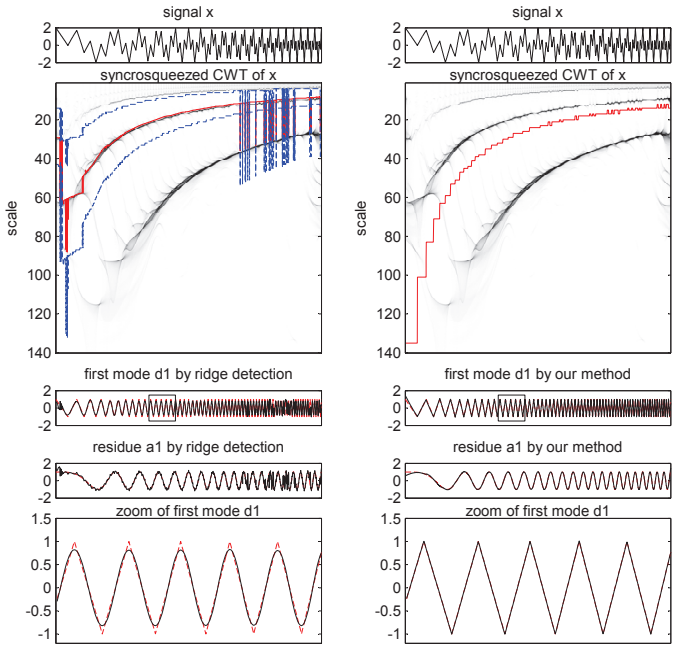

Fig. 2. Superposition of a chirp and a triangular waveform. Left panel: ridge-based method. Right panel: our proposal. Top to bottom: composed signal, synchrosqueezed CWT of the signal, and the mode and residue in black superimposed with the true components in dashed red. A zoom of the squared portion of $d_1(n)$ is shown in the last row.

such as nonlinear mode decomposition [19] and instantaneous wave shape functions [20]. A second undesire behavior of the ridge-based algorithm are the several jumps from one ridge to another present in the second half of the signal. Our algorithm, based on observed local extrema, is able to fully recover the triangular waveform because it considers the information from the finest scale to those scales defined as the distances between extrema. A zoom of the squared portion of the first mode $d_1(n)$ is shown in the last row of Fig. 2 for better appreciation.

Because the local extrema occurs at points where the signal is not differentiable, the positions of the extrema from the composed signal coincides with those of the actual mode extrema. Thus, it was not necessary to perform a local scale refinement. The mean square error is: 2.9×10^{-3}. As before, we superimposed the modes with the true components. The error for the ridge-based algorithm is: 4.9×10^{-2}.

VI. Conclusion

We developed a mode decomposition algorithm merging synchrosqueezing ideas with those of EMD's. The locality and data-driven nature of this last method which are based on the local extrema of the signal as characteristic points to define a local scale met with the solid theory behind wavelets and synchrosqueezing. The result is a method as data-driven as EMD, avoiding splines, or any kind of interpolation in the temporal domain. The choices to be made in our algorithm, such as the wavelet and its parameters are comparable to those to be made in EMD: interpolation scheme and stopping criterion.

The proposed method was successfully tested on two artificial signals with components overlapped in time and frequency. Moreover, one of the signal contained a nonlinear triangular waveform which generates several ridges in the time-scale plane. Our method was able to isolate it as a whole.

Our idea of performing an EMD decomposition in a time-scale framework should help to a better understanding of how EMD works. The problems to analyze are those which were used for pioneer analysis of EMD: two tone separation [8] and white noise decomposition [21]. It may also help to shed some light in the noise-assisted field [22]. This issues will be soon addressed in a future work.

This method should be soon tested on the most recent developments on time-scale representations such as invertible reassignment and second-order synchrosqueezing [23], or the Levenberg-Marquardt recursive synchrosqueezing [24].

Acknowledgment

This work was partially supported by PICT-ANPCYT 2012-2954, PID-UNER 6136, PIO-UNER-CONICET 146-201401-00014-CO, CITER and CONICET.

References

[1] S. Mallat, *A wavelet tour of signal processing: the sparse way*. Academic press, 2009.

[2] H.-T. Wu, Y.-H. Chan, Y.-T. Lin, and Y.-H. Yeh, "Using synchrosqueezing transform to discover breathing dynamics from ecg signals," *Applied and Computational Harmonic Analysis*, vol. 36, no. 2, pp. 354–359, 2014.

[3] X. Zhang, K. K. Lai, and S.-Y. Wang, "A new approach for crude oil price analysis based on empirical mode decomposition," *Energy economics*, vol. 30, no. 3, pp. 905–918, 2008.

[4] D. Iatsenko, P. V. McClintock, and A. Stefanovska, "Linear and synchrosqueezed time-frequency representations revisited," *Digital Signal Processing*, vol. 42, no. C, pp. 1–26, 2015.

[5] S. Meignen, T. Oberlin, and S. McLaughlin, "A new algorithm for multicomponent signals analysis based on synchrosqueezing: With an application to signal sampling and denoising," *IEEE transactions on Signal Processing*, vol. 60, no. 11, pp. 5787–5798, 2012.

[6] I. Daubechies, J. Lu, and H.-T. Wu, "Synchrosqueezed wavelet transforms: an empirical mode decomposition-like tool," *Applied and Computational Harmonic Analysis*, vol. 30, no. 2, pp. 243–261, 2011.

[7] N. E. Huang, Z. Shen, S. R. Long, M. C. Wu, H. H. Shih, Q. Zheng, N.-C. Yen, C. C. Tung, and H. H. Liu, "The empirical mode decomposition and the hilbert spectrum for nonlinear and non-stationary time series analysis," in *Proceedings of the Royal Society of London A: Mathematical, Physical and Engineering Sciences*, vol. 454, no. 1971. The Royal Society, 1998, pp. 903–995.

[8] G. Rilling and P. Flandrin, "One or two frequencies? The Empirical Mode Decomposition answers," *IEEE Transactions on Signal Processing*, vol. 56, pp. 85–95, 2008.

[9] G. Rilling, P. Flandrin, P. Goncalves *et al.*, "On empirical mode decomposition and its algorithms," in *IEEE-EURASIP workshop on nonlinear signal and image processing*, vol. 3. NSIP-03, Grado (I), 2003, pp. 8–11.

[10] G. Rilling, "Décompositions modales empiriques-contributions à la théorie, l'algorithmie et l'analyse de performances," Ph.D. dissertation, École Normale Superiéure de Lyon, France, 2007.

[11] I. Daubechies and S. Maes, "A nonlinear squeezing of the continuous wavelet transform based on auditory nerve models," *Wavelets in medicine and biology*, pp. 527–546, 1996.

[12] F. Auger and P. Flandrin, "Improving the readability of time-frequency and time-scale representations by the reassignment method," *IEEE Transactions on Signal Processing*, vol. 43, no. 5, pp. 1068–1089, 1995.

[13] E. Brevdo and H. Wu, "The synchrosqueezing toolbox," 2011.

[14] E. Brevdo, N. S. Fuckar, G. Thakur, and H.-T. Wu, "The synchrosqueezing algorithm: a robust analysis tool for signals with time-varying spectrum," *Arxiv preprint*, 2011.

[15] P. Flandrin and P. Goncalves, "Empirical mode decompositions as data-driven wavelet-like expansions," *International Journal of Wavelets, Multiresolution and Information Processing*, vol. 2, no. 04, pp. 477–496, 2004.

[16] T. Oberlin, S. Meignen, and V. Perrier, "An alternative formulation for the empirical mode decomposition," *IEEE Transactions on Signal Processing*, vol. 60, no. 5, pp. 2236 –2246, may 2012.

[17] N. Pustelnik, P. Borgnat, and P. Flandrin, "Empirical mode decomposition revisited by multicomponent non-smooth convex optimization," *Signal Processing*, vol. 102, pp. 313–331, 2014.

[18] A. Linderhed, "Image empirical mode decomposition: A new tool for image processing," *Advances in Adaptive Data Analysis*, vol. 1, no. 02, pp. 265–294, 2009.

[19] D. Iatsenko, P. V. McClintock, and A. Stefanovska, "Nonlinear mode decomposition: A noise-robust, adaptive decomposition method," *Physical Review E*, vol. 92, no. 3, p. 032916, 2015.

[20] H.-T. Wu, "Instantaneous frequency and wave shape functions (i)," *Applied and Computational Harmonic Analysis*, vol. 35, no. 2, pp. 181–199, 2013.

[21] P. Flandrin, G. Rilling, and P. Goncalves, "Empirical mode decomposition as a filter bank," *IEEE Signal Processing Letters*, vol. 11, no. 2, pp. 112–114, 2004.

[22] Z. Wu and N. E. Huang, "Ensemble empirical mode decomposition: a noise-assisted data analysis method," *Advances in Adaptive Data Analysis*, vol. 1, no. 01, pp. 1–41, 2009.

[23] T. Oberlin, S. Meignen, and V. Perrier, "Second-order synchrosqueezing transform or invertible reassignment? towards ideal time-frequency representations," *IEEE Transactions on Signal Processing*, vol. 63, no. 5, pp. 1335–1344, 2015.

[24] D. Fourer, F. Auger, and P. Flandrin, "Recursive versions of the Levenberg-Marquardt reassigned spectrogram and of the synchrosqueezed stft," in *IEEE Int. Conf. on Acoust., Speech and Signal Proc. ICASSP-16, Shanghai (PRC).* IEEE, 2016, p. to appear.